Archives of Hydro-Engineering and Environmental Mechanics
Vol. 54 (2007), No. 3, pp. 183–206
© IBW PAN, ISSN 1231–3726

A Study on Pre-Failure Deformations of Granular Soils

Andrzej Sawicki

Institute of Hydro-Engineering Polish Academy of Sciences,
ul. Kościerska 7, 80-328 Gdańsk, Poland, e-mail: as@ibwpan.gda.pl

(Received September 11, 2007)

Abstract

A simple model describing pre-failure deformations of granular soils is derived on the basis of a wide range of experimental data. The model is defined by two incremental equations describing the volumetric and deviatoric strains. Functions appearing in governing equations were determined from experiments performed in the triaxial apparatus, with additional measurements of lateral strains for some simple stress paths. These functions are different for loading and unloading, and have different shapes for contractive and dilative soil samples. The instability line is built into the structure of the model. The incremental equations were applied to predict the soil behaviour during anisotropic compression, including determination of the K_0-line. Some basic statistical characteristics of the initial density index of investigated soils and deformations during isotropic compression are presented.

Key words: granular soils, pre-failure deformations, instability line

1. Introduction

This paper is about strains that develop in granular soils before failure. This problem is still one of the central points in contemporary soil mechanics and, in spite of extensive research, has not yet been solved satisfactorily. The main stream of research is based on the elasto-plastic methodology, which, however, is more and more a subject of criticism, see Bolton (2000, 2001) or Kolymbas (2000a). The basic objections deal with intricacy of those models and with the lack of satisfactory agreement with experimental results, see Saada & Bianchini (1989), or more recently Sawicki (2003).

Even some authors of elasto-plastic models admit that they are mostly useful as "students models", due to their "nice structure", after Wood (1990). Also some alternatives to elasto-plasticity as, for example, hypoplasticity (Kolymbas 2000b) are still far from ideal, see Głębowicz (2006). This subject certainly needs further extensive investigations in order to elaborate effective models describing deformations of granular media.

Some attempt, differing from those widely applied in geotechnical literature, is presented in this paper. The starting point to theoretical considerations is a great amount of experimental data, obtained for a model sand "Skarpa", investigated in a modern triaxial apparatus that enables a measurement of both vertical and lateral strains developing for various stress paths. These data have been analysed within the framework of the most simple theoretical structure, i.e. the system of incremental equations describing increments of volumetric and deviatoric strains as functions of given stress histories. Theoretical model takes into account the initial structure of granular medium, that is defined either as contractive or dilative. Considerations presented in the present paper relate to either dry or saturated soils but with free drainage of pore water allowed (zero pore pressure). This means that the global stresses are equal to effective stresses in this case. The undrained behaviour of "Skarpa" sand will be analysed in a separate paper.

In the second section of this paper, the program of experimental research is briefly described. The third section deals with the theoretical model of soil deformations, which is defined by a system of incremental equations, formulated separately for loading and unloading. In traditional plasticity, the definition of loading and unloading depends on the orientation of the stress increment with respect to the yield/loading surface in the stress space, which leads to misunderstandings, as the same stress increment may be considered as loading or unloading, depending on the shape of yield surface assumed. In this paper, we propose a new definition of loading and unloading which is more objective. Subsequent sections deal with the isotropic compression and shearing at constant mean stress of soil samples. These tests allow for calibration of incremental equations, i.e. for determination of some material parameters. Then, predictions of the model are compared with experimental data for a loading path different from those used in calibration of the model, designated as the anisotropic compression path. The problem of K_0 line is discussed on the basis of the results obtained. Finally, some statistical considerations regarding accuracy of experimental calibration/verification are presented.

2. Experimental Programme

An extensive experimental program has been performed in the geotechnical laboratory of the Institute of Hydro-Engineering in order to study the pre-failure behaviour of granular soils. The experiments were performed in a computer controlled hydraulic triaxial testing system from GDS Instruments, see Menzies (1988), Świdziński & Mierczyński (2002). The system has additionally been equipped with special gauges enabling the local measurement of both lateral and vertical strains which are more precise than traditional techniques.

The experiments were performed mainly on the model sand "Skarpa", composed of quartz grains of a median size 420 μm and uniformity coefficient of 2.5. The specific gravity is 2.65. This sand has a maximum void ratio of 0.677 and minimum void ratio of 0.432. The angles of internal friction for loose (I_D = density index = 0.15) and dense sand (I_D = 0.87) are 34° and 41° respectively. The soil samples

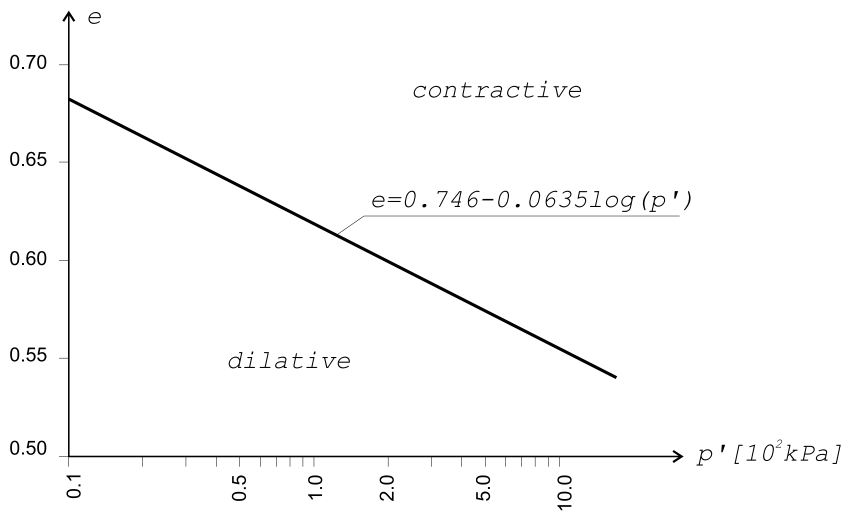

Fig. 1. Steady state line for "Skarpa" sand, after Świdziński & Mierczyński (2005)

were prepared in a membrane-lined split moulder either by moist tampling or by water pluviation methods. The first method assured an achievement of relatively uniform, very loose samples which revealed contractive behaviour when sheared, and the second one, uniformity of denser samples exhibiting a dilative character, see Świdziński & Mierczyński (2005).

Świdziński & Mierczyński (2005) have determined the steady state line for "Skarpa" sand, by performing a large number of drained and undrained experiments. Recall that Poulos (1981) defined the steady state of deformation of granular medium as the state when the soil is continuously deforming at constant volume, constant mean and shear stresses, as well as constant velocity. We do not discuss, in the present paper, some shortcomings of the Poulos definition which contradicts the Newtonian mechanics (for example, the material body moves with constant velocity only when the resultant force acting on this body is equal to zero), but accept at present a general concept of the steady state. The steady state line divides the plane e, p' (p' in logarithmic scale), where e = void ratio, p' = effective mean pressure, into two parts as shown in Fig. 1 in semi-logarithmic scale. The region above the steady state line (SSL) represents the states of granular medium corresponding to contractive behaviour during shearing, whilst the states below this line correspond to dilative behaviour. These behaviours will be described in detail in subsequent sections. SSL for "Skarpa" sand is defined by the following equation:

$$e = 0.746 - 0.0635 \log (p'), \tag{1}$$

where p' is expressed in kPa.

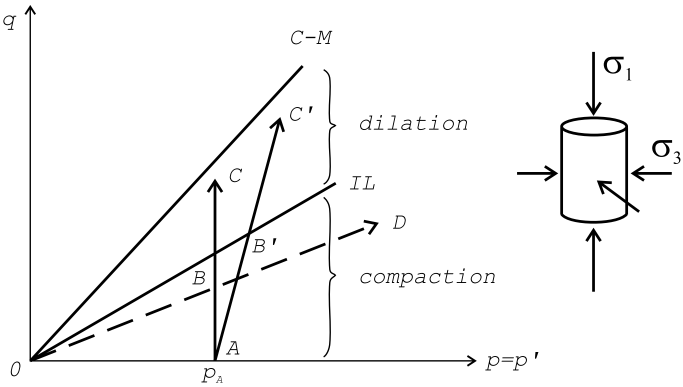

Fig. 2. Instability line (IL) and compaction/dilation zones in the stress space

Świdziński & Mierczyński (2005) have also determined experimentally the instability line (IL) for "Skarpa" sand, which is a very important characteristic of granular media, see also Sladen et al (1985), Lade (1992). This importance is manifested in experiments performed on both, dry and water saturated soils. In the case of dry sands, or water saturated but with free drainage of pore water allowed, IL divides the region, in the admissible effective stress space, onto the regions of contractive and dilative behaviours (for dilative soils) as shown in Fig. 2.

In the case of triaxial compression tests, considered in this paper, the stress invariants are defined as follows:

$$p' = p = \frac{1}{3}(\sigma_1 + 2\sigma_3), \tag{2}$$

$$q = \sigma_1 - \sigma_3, \tag{3}$$

where: p' = effective mean pressure = p = total mean pressure; q = deviatoric stress; σ_1 = vertical stress = σ_1' = effective vertical stress; σ_3 = lateral stress = σ_3' = effective lateral stress.

Instability line is given by the following equation:

$$q = \Psi p', \tag{4}$$

where the average value of $\Psi = 0.98$, but this parameter varies from 0.8 to 1.05.

Dilative sand during shearing first compacts (paths AB or AB′ in Fig. 2) and then dilates (paths BC or BC′ in Fig. 2). In the case of undrained conditions, not discussed in the present paper, IL corresponds to the maximum shear stress that can be supported by the saturated sand. Note that IL is located inside a region bounded by the Coulomb-Mohr failure line, that is given by the following equation, for the triaxial compression tests:

$$q = \frac{6\sin\varphi}{3-\sin\varphi}p' = \Phi p', \tag{5}$$

where φ = angle of internal friction.

The experimental program included investigation of various samples of "Skarpa" sand, characterized by different initial states, loaded along various stress paths, as schematically shown in Fig. 2. We have used the results obtained for the stress path OABC for calibration of the incremental model. Results obtained for other stress paths (as OD) served for verification of the model. The data presented in subsequent sections correspond to mean values of respective quantities. Some statistical analysis of experimental data is presented in Section 7.

3. Incremental Model of Soil Deformations

Basic Definitions

The stresses have already been defined in Section 2, as well as some basic characteristics of granular soils as the Coulomb-Mohr failure condition and instability line. During the experiments, the local strains were measured, defined as follows: ε_1 = vertical strain; ε_3 = horizontal strain. The soil mechanics sign convention is used, which means that compression is positive. The following strain invariants are introduced:

$$\varepsilon_v = \varepsilon_1 + 2\varepsilon_3, \tag{6}$$

$$\varepsilon_q = \frac{2}{3}(\varepsilon_1 - \varepsilon_3). \tag{7}$$

Note that $\varepsilon_v = \operatorname{tr} \boldsymbol{\varepsilon}$; $\boldsymbol{\varepsilon}$ = Cauchy strain tensor, denotes volumetric deformation of soil sample, that is also the first invariant of the strain tensor. The quantity ε_q denotes the deviatoric strain, which is related to the second invariant of strain deviator, defined as follows:

$$K_2 = \frac{1}{3}\operatorname{tr}\left(\boldsymbol{\varepsilon}^{dev}\right)^2; \quad \boldsymbol{\varepsilon}^{dev} = \boldsymbol{\varepsilon} - \frac{1}{3}\operatorname{tr}\boldsymbol{\varepsilon}\cdot\mathbf{1}. \tag{8}$$

There is:

$$\varepsilon_q = \sqrt{\frac{4}{3}K_2}. \tag{9}$$

Also note that the quantities p and q, introduced in the previous section, are directly related to respective invariants of the stress tensor $\boldsymbol{\sigma}$ (which is equal to the effective stress tensor in the case analysed), i.e.

$$q = \sqrt{3J_2}, \tag{10}$$

$$J_2 = \frac{1}{2}\mathrm{tr}\left(\boldsymbol{\sigma}^{dev}\right)^2 = \text{ second invariant of the stress deviator,} \tag{11}$$

$$\boldsymbol{\sigma}^{dev} = \boldsymbol{\sigma} - \frac{1}{3}\mathrm{tr}\boldsymbol{\sigma}\cdot\mathbf{1}, \tag{12}$$

$$p = I_1 = \frac{1}{3}\mathrm{tr}\boldsymbol{\sigma} = \text{ first invariant of the stress tensor } = \text{ mean or spherical stress.} \tag{13}$$

An important problem is the definition of loading and unloading, cf. Życzkowski (1973). Recall that, according to classical knowledge, during loading, both the elastic and plastic strains develop in the material, whilst during unloading the elastic strains are recovered. In elasto-plasticity, the process of loading/unloading is defined by the orientation of the stress increment $d\sigma$ with respect to the assumed yield surface. If this increment is directed outwards to the current yield surface, the process of loading takes place. If it is directed inwards, the process of unloading takes place. If it is directed inwards, the process of unloading occurs. Such a definition may lead to some inconsistencies, as the definition of loading/unloading depends on details of particular elasto-plastic model. Therefore, the same stress increment may be associated with loading in the case of a certain model, whilst for another model, this increment may be associated with unloading, see Sawicki (2003).

In order to avoid such controversy, we propose a simple definition of loading/unloading, which is independent on the choice of particular yield surface, related to a specific elasto-plastic model. This definition follows from the decomposition of the stress and strain tensors onto spherical and deviatoric parts. Therefore, we can define separately the spherical and deviatoric loading/unloading in a simple manner, depending on the sign of stress increments dp and dq. Recall that positive sign denotes compression. According to the above considerations, we have:

- spherical loading when $dp > 0$;
- spherical unloading when $dp < 0$;
- deviatoric loading when $dq > 0$;
- deviatoric unloading when $dq < 0$.

Incremental Equations

A general form of incremental equations describing the spherical and deviatoric strain increments is the following:

$$d\varepsilon_v = M dp + N dq, \tag{14}$$

$$d\varepsilon_q = P dp + Q dq, \tag{15}$$

where M, N, P, Q are functions which may depend on the stress and strain invariants. At present, we do not impose any other restrictions on these functions.

According to the definition of loading/unloading, the above functions should have different shapes for loading and unloading. Therefore, the following definitions are assumed:

- if $dp > 0$ then $M = M_l$ and $P = P_l$;
- if $dp < 0$ then $M = M_u$ and $P = P_u$;
- if $dq > 0$ then $N = N_l$ and $Q = Q_l$;
- if $dq < 0$ then $N = N_u$ and $Q = Q_u$;

where the subscript "*l*" denotes the shape of respective function during loading, and the subscript "*u*" respective shape for unloading. We assume that specific shapes of functions $(\ )_l$ and $(\ )_u$, where $(\ ) = M, N, P, Q$, should be determined experimentally for the loading and unloading along the stress paths OABC, see Fig. 2. The results of experiments performed for other stress paths should serve for verification of the most simple incremental model proposed in this paper.

In elasto-plasticity, equations describing the increments of plastic strains are determined by differentiation of the function designated as the plastic potential, and increments of elastic strains are given by respective physical law as, for example, Hooke's law. The total strain increment is a sum of elastic and plastic strain increments. In the present paper, the development of total strains is studied, although some comparisons with elasto-plastic interpretation of these strains are sometimes made.

Note that in most engineering models isotropy of material is assumed. For example, in the case of isotropic elastic material (linear or non-linear), the functions N and P in Eqs. (14) and (15) should be assumed zero, as the volumetric strain may be caused only by the mean stress and the deviatoric strain only by the shear stress. Granular media display features which cannot occur in other materials as, for example, volumetric changes due to shearing. Therefore, it should be $N \neq 0$ in Eq. (14). The function P was introduced in Eq. (15) as some deviatoric strains caused purely by the mean stress were observed in experiments. This means that the samples investigated display some anisotropic features, in spite of very careful preparation of them before the experiment.

Stress and Strain Units

During analysis of experimental data, presented in subsequent sections, we have introduced very convenient stress and strain units, namely:

- stress unit = 10^5 N/m^2 = 0.1 MPa;
- strain unit = 10^{-3} (non-dimensional).

This means that the stress invariants p and q will be expressed in unit 10^5 N/m^2, and respective strains ε_v and ε_q in unit 10^{-3}. For example, if $p = 3 \times 10^5$ N/m^2 we substitute into respective equation just $p = 3$, etc. This is equivalent to the introduction of non-dimensional quantities as p = real mean stress/stress unit, ε_v = real volumetric strain/strain unit, etc.

4. Isotropic Compression

During the isotropic compression (path OA in Fig. 2) only the mean stress increases, whilst the stress deviator's equal to zero. Fig. 3a shows ε_v, p curves for loading (path OA) and unloading (path AO). This is an idealized diagram, illustrating the qualitative behaviour of investigated sand during a single cycle of virgin compression and subsequent unloading. Such a behaviour does not depend on the initial state of soil, i.e. is similar to initially loose and dense samples.

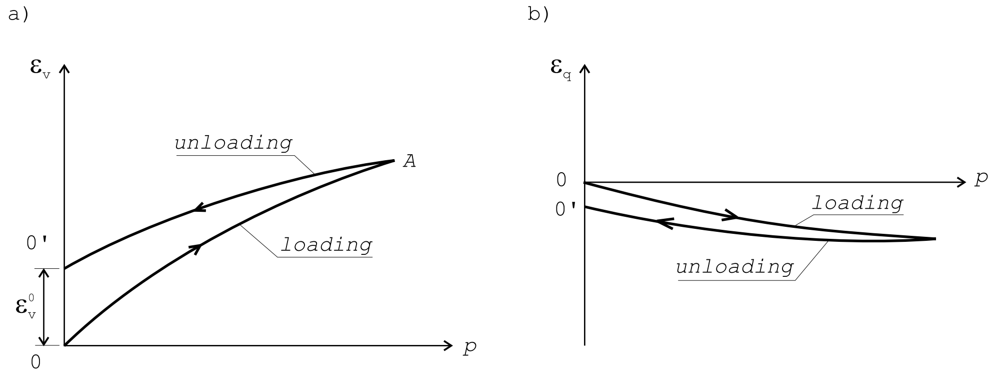

Fig. 3. Development of volumetric (a) and deviatoric (b) strains during a single cycle of isotropic loading and unloading

During isotropic compression, the deviatoric strains also develop, which is a characteristic feature of anisotropic materials, see Fig. 3b. Recall, that for initially isotropic soil there should be $\varepsilon_q = 0$. It is very difficult to prepare isotropic samples for laboratory investigations.

The loading curve OA shown in Fig. 3a, can be approximated by various mathematical formulae. We have found that a good approximation gives the following formula:

$$\varepsilon_v = A_v \sqrt{p}, \tag{16}$$

where A_v = coefficient that characterizes compressibility of sand, that depends on the initial density of soil. Formula (16) is convenient for two reasons. First, there appears a single coefficient only. Secondly, it can be rewritten as:

$$p = \frac{\sqrt{p}}{A_v}\varepsilon_v = K(p)\,\varepsilon_v, \tag{17}$$

where $K(p)$ = coefficient of compressibility which depends on the mean effective pressure, in the form commonly used in soil mechanics. Differentiation of Eq. (16) leads to the following formula:

$$d\varepsilon_v = \frac{A_v}{2\sqrt{p}} dp = M_l dp. \tag{18}$$

The unloading curve (A0′ in Fig. 3a) can be approximated by a similar formula, namely:

$$\varepsilon_v = \varepsilon_v^o + A_v^u \sqrt{p}, \tag{19}$$

where ε_v^o = permanent (plastic) strain after unloading to $p = 0$. Differentiation of the above equation leads to the following formula:

$$d\varepsilon_v = \frac{A_v^u}{2\sqrt{p}} dp = M_u dp. \tag{20}$$

Similar technique can be applied to describe the deviatoric strains that develop during a single cycle of isotropic loading and unloading, see Fig. 3b. The final results are the following:

$$d\varepsilon_q = \frac{A_q}{2\sqrt{p}} dp = P_l dp \text{ during loading;} \tag{21}$$

$$d\varepsilon_q = \frac{A_q^u}{2\sqrt{p}} dp = P_u dp \text{ during unloading.} \tag{22}$$

Table 1 shows average coefficients A_v and A_q for "Skarpa" sand determined experimentally for initially loose and dense samples. Some statistical analysis of these coefficients will be presented in Section 7.

Table 1. Average material parameters describing isotropic compression of "Skarpa" sand, for initially loose and dense samples

Initial I_D	A_v	A_v^u	A_q	A_q^u
Loose 0.02–0.44	6.01	4.41	–0.905	–0.447
Dense 0.71–0.86	3.47	2.91	–0.47	–0.205

Recall that these coefficients correspond to stress and strain units, already introduced in Section 3. For example, if $p = 3 \times 10^5$ N/m^2, we introduce into Eq. (16) the multiplier 3 and obtain for loose sand $\varepsilon_v = A_v \sqrt{p} = 6.01\sqrt{3} = 10.41$, expressed in strain unit. This means that the real volumetric strain is $10.41 \times 10^{-3} \cong 0.0104$.

5. Shearing at Constant Mean Stress

Shearing at constant mean stress is realized on the stress path ABC, see Fig. 2. Experiments were performed at various values of $p = p_A = \text{const}$, and for this reason a special method of interpretation of empirical data should be found, that would enable a common interpretation of the whole set of these data. We have found that interpretation of experimental data on the $\varepsilon_v \big/ \sqrt{p} - \eta = q/p$ and $\varepsilon_q \big/ \sqrt{p} - \eta$ planes is quite useful, as it enables presentation of different experimental curves (obtained for various values of p) as roughly single curves. Obviously, it is not the only method of presentation of experimental data, but for working purposes such a method seems to be sufficiently good.

In the case of shearing of granular media, it is important to distinguish between contractive or dilative behaviours. According to the present state of knowledge, the granular soils characterized by the initial state lying above the steady state line (see Fig. 1) display contractive behaviour, whilst the initial states below this line characterize the dilative soils. At present, there is no experimental evidence or strong theoretical arguments to reject this important division. Therefore, we shall present the experimental data separately for initially dilative and contractive soils.

Dilative Soils – Volumetric Changes Due to Shearing

Fig. 4 shows a typical diagram illustrating the volumetric changes due to shearing in the dilative sand. This diagram may be treated as averaged common curve for various experimental data, obtained for different values of p. Obviously, the results of particular experiments differ quantitatively from this "model curve", which is a characteristic feature of granular media. Some statistical considerations are presented in Section 7.

During the first stage of shearing (path AB), the volumetric strain increases (compaction), and approximately at point B corresponding to the instability line ($\eta = \eta'$), the process of dilation begins. The stress-strain curve approaches the vertical line $\eta = \eta''$, that corresponds to the Coulomb-Mohr failure criterion ($\eta'' = \Phi$, see Eq. 5). A good approximation of experimental results is given by the following polynomials:

$$\varepsilon_v = \sqrt{p}\left(a_1\eta^2 + a_2\eta\right) \text{ for } \eta \in \langle 0, \eta' \rangle, \tag{23}$$

$$\varepsilon_v = \sqrt{p}\left(a_3\eta^2 + a_4\eta + a_5\right) \text{ for } \eta \in \langle \eta', \eta'' \rangle, \tag{24}$$

where a_i are certain coefficients, which should ensure the continuity of this approximation at point $\eta = \eta'$ (the same volumetric strain and the same first derivative). For the averaged experimental data we have: $a_1 = -1.458$; $a_2 = 2.39$; $a_3 = -42.215$; $a_4 = 69.232$; $a_5 = -27.405$. Recall respective units! The path ABC corresponds to loading, according to the definition adapted in this paper, as $dq > 0$, see Fig. 2.

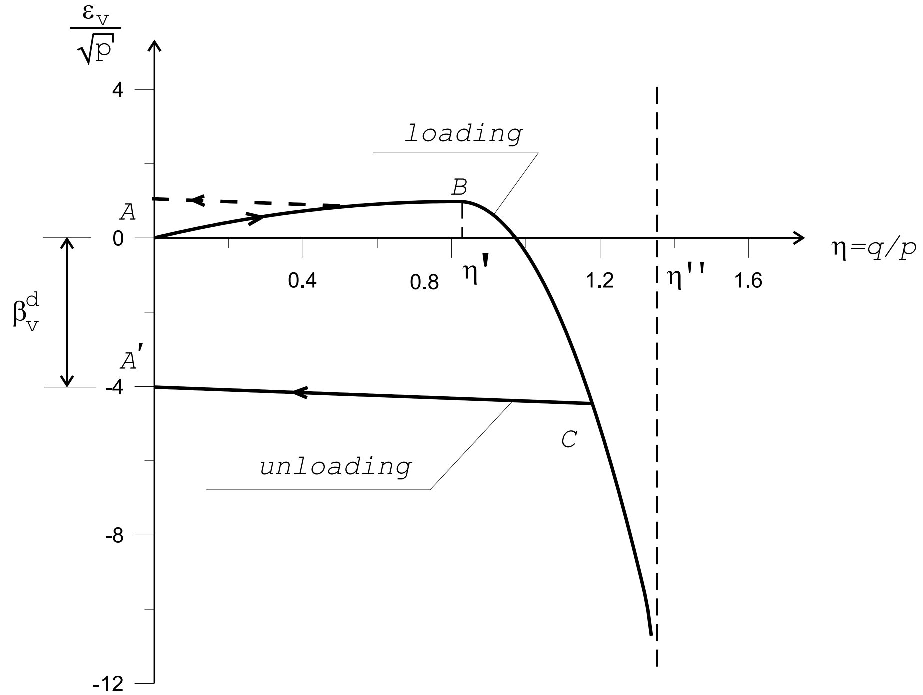

Fig. 4. Volumetric changes due to shearing for dilative "Skarpa" sand. See stress path ABC in Fig. 2

Differentiation of Eqs. (23) and (24) with respect to q leads to the following incremental equations:

$$d\varepsilon_v = \frac{1}{\sqrt{p}}\left(2a_1\eta + a_2\right)dq = N_l dq \text{ for } \eta \in \langle 0, \eta' \rangle, \tag{25}$$

$$d\varepsilon_v = \frac{1}{\sqrt{p}}\left(2a_3\eta + a_4\right)dq = N_l dq \text{ for } \eta \in \langle \eta', \eta'' \rangle. \tag{26}$$

During unloading, for example path CA′, the stress-volumetric strain path can be treated as approximately linear, see Fig. 4:

$$\frac{\varepsilon_v}{\sqrt{p}} = a_v^d \eta + \beta_v^d, \tag{27}$$

where β_v^d = permanent (plastic) volumetric strain divided by the square root of mean stress after deviatoric unloading. Differentiation of Eq. (27) with respect to q gives the following incremental equation:

$$d\varepsilon_v = \frac{1}{\sqrt{p}} a_v^d dq = N_u dq, \tag{28}$$

where $a_v^d = -0.376$ for the "Skarpa" sand.

Note that during deviatoric unloading the dilative sand densifies.

Dilative Soils – Deviatoric Deformation Due to Shearing

The averaged deviatoric deformation of dilative soil due to shearing along path ABC (see Fig. 2) is shown in Fig. 5. This deformation increases up to $\eta = \eta''$ corresponding to the Coulomb-Mohr failure criterion, and the role of instability line is not displayed in this case, in contrast to volumetric deformation (Fig. 4).

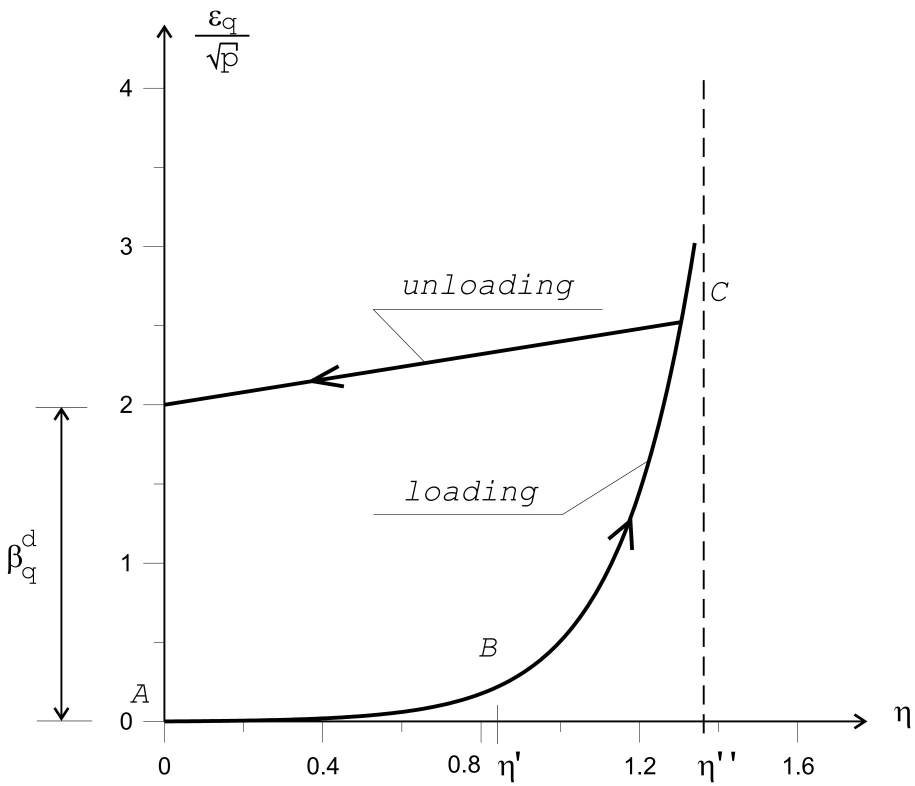

Fig. 5. Deviatoric deformation of dilative sand "Skarpa" due to shearing (stress path ABC in Fig. 2). Similar curves are obtained for contractive sand

The behaviour shown in Fig. 5 can be approximated by the following function:

$$\frac{\varepsilon_q}{\sqrt{p}} = b_1[\exp(b_2\eta) - 1], \tag{29}$$

where $b_1 = 2.671 \times 10^{-3}$ and $b_2 = 5.248$ (recall respective units!). Differentiation of this equation with respect to q leads to the following incremental equation:

$$d\varepsilon_q = \frac{b_1 b_2}{\sqrt{p}} \exp(b_2 q)\, dq = Q_l dq. \tag{30}$$

During unloading (path CBA in Fig. 2), the stress-strain characteristic is almost linear, and can be approximated by the following equation:

$$\frac{\varepsilon_q}{\sqrt{p}} = b_q \eta + \beta_q^d, \tag{31}$$

where $b_q = 0.399$ and b_q^d = permanent normalized deviatoric strain (see Fig. 5). Differentiation of Eq. (30) with respect to q leads to the following incremental equation:

$$d\varepsilon_q = \frac{1}{\sqrt{p}} b_q dq = Q_u dq. \tag{32}$$

Contractive Soils – Volumetric Changes Due to Shearing

Fig. 6 illustrates the volumetric changes of contractive "Skarpa" sand. Note that this behaviour is different from that characteristic of dilative samples, cf. Fig. 4, as the contractive sample continuously densifies when sheared.

A good approximation of the behaviour shown in Fig. 6 gives the following equation:

$$\frac{\varepsilon_v}{\sqrt{p}} = c_1 \eta^4, \tag{33}$$

where $c_1 = 3.4$ for our experimental data. Differentiation of Eq. (33) with respect to q gives:

$$d\varepsilon_v = \frac{4c_1}{\sqrt{p}} \eta^3 dq = N_l dq. \tag{34}$$

During the unloading, the stress-strain curve is almost linear, and can be approximated by the following formula:

$$\frac{\varepsilon_v}{\sqrt{p}} = a_v^c \eta + \beta_v^c, \quad d\varepsilon_v = \frac{a_v^c}{\sqrt{p}} dq = N_u dq, \tag{35}$$

where $a_v^c = -0.87$ and β_v^c is a normalized plastic volumetric strain, shown in Fig. 6. Note, that during unloading the contractive sample densifies as during loading.

Contractive Soils – Deviatoric Deformation Due to Shearing

The qualitative character of deviatoric deformation of contractive soil due to shearing is similar to that shown in Fig. 5. We assume the stress-strain approximation also similar to Eq. (29), but with different coefficients:

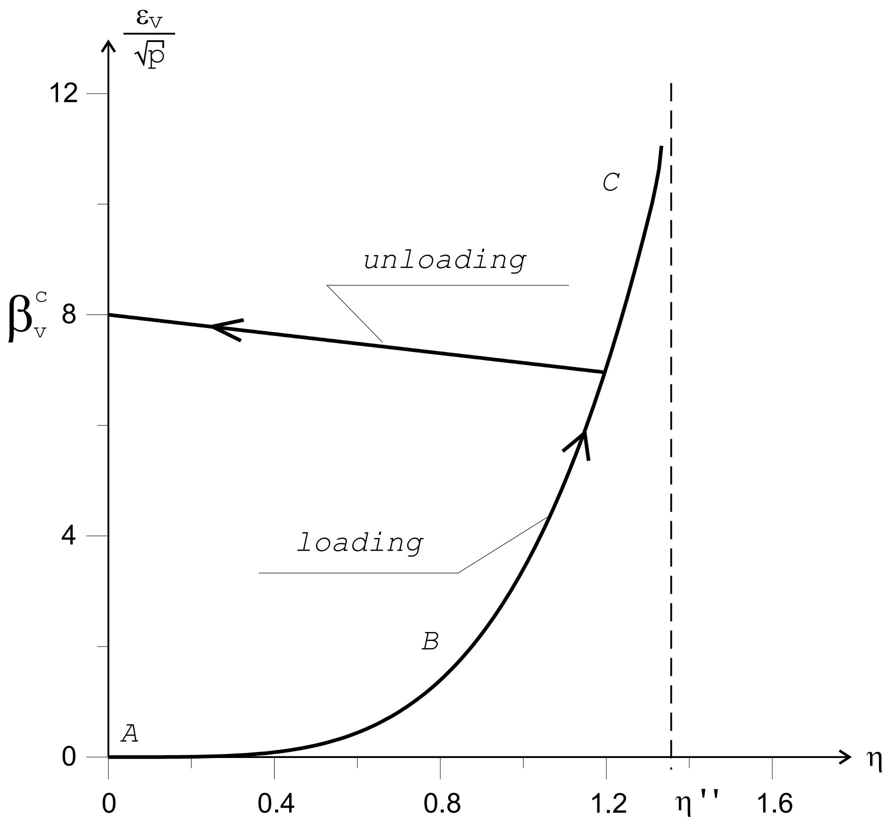

Fig. 6. Volumetric changes of contractive "Skarpa" sand due to shearing

$$\frac{\varepsilon_q}{\sqrt{p}} = g_1[\exp(g_2\eta) - 1], \tag{36}$$

where $g_1 = 0.0206$ and $g_2 = 4.587$. Respective incremental equation is the following:

$$d\varepsilon_q = \frac{g_1 g_2}{\sqrt{p}} \exp(g_2\eta)\, dq = Q_l dq. \tag{37}$$

Respective incremental equation for unloading is similar to Eq. (32):

$$d\varepsilon_q = \frac{1}{\sqrt{p}} g_q dq = Q_u dq, \tag{38}$$

where $g_q = 0.76$.

6. Anisotropic Compression and K_0-Line

In this section, we shall predict the soil deformations for anisotropic compression (path OD in Fig. 2) using previously derived incremental equations. Their general form is given in Eqs. (14) and (15), and the shape of respective function appearing in these equations (M, N, P, Q) depends on the initial state of soil sample (i.e. dilative or contractive), and on whether the respective stress increment corresponds to loading or unloading.

Loading of Dilative Soil

In the case of loading of the dilative soil, the respective functions are given in Eqs. (18, 21, 25) or (26) and (30). Consider the case then the slope of stress path OD (see Fig. 2) is smaller than the slope of instability line, therefore respective functions are given by Eqs. (18, 21, 25) and (30). Substitution of these functions into Eqs. (14) and (15) leads to the following specific form of incremental equations describing deformations of the soil sample:

$$d\varepsilon_v = \frac{A_v}{2\sqrt{p}}dp + \frac{1}{\sqrt{p}}\left(2a_1\eta + a_2\right)dq, \tag{39}$$

$$d\varepsilon_q = \frac{A_q}{2\sqrt{p}}dp + \frac{b_1 b_2}{\sqrt{p}}\exp\left(b_2\eta\right)dq, \tag{40}$$

where average values of the coefficients have already been presented after respective formulae. The anisotropic compression is defined by the following stress path:

$$q = \alpha p, \tag{41}$$

where $0 < \alpha \leq \eta'$ is the case considered. Because $\eta = \alpha$ and $dq = \alpha dp$, Eqs. (39) and (40) simplify:

$$d\varepsilon_v = \frac{1}{\sqrt{p}}\left[\frac{A_v}{2} + \left(2a_1\alpha + a_2\right)\alpha\right]dp = \frac{C_v}{\sqrt{p}}dp, \tag{42}$$

$$d\varepsilon_q = \frac{1}{\sqrt{p}}\left[\frac{A_q}{2} + \alpha b_1 b_2 \exp\left(b_2\alpha\right)\right]dp = \frac{C_q}{\sqrt{p}}dp, \tag{43}$$

where: $A_v = 3.47$; $A_q = -0.47$; $a_1 = -1.458$; $a_2 = 2.39$; $b_1 = 0.00267$; $b_2 = 5.248$. For the case considered, we have:

$$C_v = -2.916\alpha^2 + 2.39\alpha + 1.735, \tag{44}$$

$$C_q = -0.235 + 0.014\alpha\exp\left(5.248\alpha\right). \tag{45}$$

Integration of Eqs. (42) and (43), with zero initial conditions, leads to the following formulae for the volumetric and deviatoric strains that develop during anisotropic compression:

$$\varepsilon_v = 2C_v \sqrt{p}, \tag{46}$$

$$\varepsilon_q = 2C_q \sqrt{p}. \tag{47}$$

For example, for $\alpha = 0.727$ one obtains $\varepsilon_v = 3.863\sqrt{p}$ and $\varepsilon_q = 0.8\sqrt{p}$.

Loading of Contractive Soil

Consider the volumetric changes of contractive soil. From Eqs. (18) and (34) one obtains the following incremental equation:

$$d\varepsilon_v = \frac{1}{\sqrt{p}}\left[\frac{A_v}{2} + 4c_1\alpha^4\right]dp = \frac{1}{\sqrt{p}}C_v' dp, \tag{48}$$

where $A_v = 6.01$ and $c_1 = 3.4$. For $\alpha = 0.39$ one obtains $\varepsilon_v = 6.64\sqrt{p}$. The experiment performed for contractive soil gives $\varepsilon_v = 7.34\sqrt{p}$. Note that in this case, the difference between theoretical prediction and experimental results is 9.5% . But also note that we have used the average values of A_v and c_1 for predicting the results of a single experiment performed on a sample which might have different characteristics A_v and c_1. Many realistic combinations of the coefficients, close to their averages, may give "ideal agreement" between analytical prediction and experimental result as, for example, $A_v = 6.71$ and $c_1 = 3.4$.

The above exercise illustrates the basic problem that appears in soil mechanics, namely a proper experimental verification of theoretical models. All the coefficients (sometimes designated as "material constants") characterising these various models are of statistical nature. There still do not exist rational criteria enabling assessment of conformity of various theoretical predictions with empirical data. Some considerations about this matter will be presented in Section 7.

K_0-Line

The coefficient of earth pressure at rest K_0 corresponds to a very important practical case when the horizontal strain equals zero, as appears, for example, in a half-space built of granular soil where lateral displacements are prevented. In the case of triaxial tests, this coefficient is defined as:

$$K_0 = \frac{\sigma_3}{\sigma_1} \text{ for } \varepsilon_3 = 0. \tag{49}$$

From Eqs. (6) and (7) it follows:

$$\varepsilon_1 = \frac{1}{3}\varepsilon_v + \varepsilon_q, \tag{50}$$

$$\varepsilon_3 = \frac{1}{3}\varepsilon_v - \frac{1}{2}\varepsilon_q. \tag{51}$$

It follows from Eqs. (49) and (51) that, on the K_0-line in the stress space, there should be:

$$2C_v - 3C_q = 0, \tag{52}$$

where, for example, C_v and C_q are given by Eqs. (45) and (46) for dilative soil. Substitution of these relations into Eq. (52) leads to an equation for determination of the coefficient α corresponding to K_0 conditions. The solution is following $\alpha = \alpha_0 = 0.884 = K_0$. The above result means that the K_0-line can be determined analytically, just knowing the volumetric and deviatoric deformations caused by the stress paths OA and ABC (see Fig. 2). It is believed that this is an original result, quite different from the Jaky formula commonly used in soil mechanics (see Craig 1987):

$$K_0 \cong 1 - \sin\varphi. \tag{53}$$

Note that Eq. (53) relates directly the coefficient K_0 to the strength characteristics as the angle of internal friction, whilst the approach presented in this Section shows the links of K_0 with deformation characteristics. This latter case is based on more solid physical ground as the definition of K_0 is based on the deformation criterion, see Eq. (49). Obviously, the problem of K_0 is more complex as this coefficient also depends on the loading history but more extensive discussion on this problem is beyond the scope of the present paper (see Sawicki 1994).

Also note that the obtained value of K_0 is close to the value of η' describing the instability line. Available experimental data, although quite rich, do not allow for deeper analysis on this problem, particularly as they have a statistical nature.

7. Some Statistical Considerations

Experimental data presented in previous sections illustrate the pre-failure behaviour of granular soils, mainly from the qualitative point of view. Respective parameters ("material constants"), which appear in incremental equations, are some averages calculated from available empirical data. Therefore, already presented results describe some "model sand Skarpa" using deterministic methods, as commonly accepted in soil mechanics. In fact, all the parameters appearing in soil mechanics models are of statistical nature, and not much attention is devoted to this important problem in geotechnical literature. Probably, it is the main reason of so extensive a production of various models, which continuously fail to pass empirical verifications, whatsoever that means (cf. literature quoted in Introduction).

In this Section, we would like to draw attention just only to a couple of problems, which are of fundamental importance for the proper description of mechanical behaviour of granular soils. The first one deals with the statistical character of the initial state of soil sample. The second deals with deformation characteristics of granular soils during isotropic compression.

Initial State of Soil

Initial state of granular soils is traditionally classified using a single parameter, designated as the density index I_D (or relative density D_r which means the same), cf. Lambe & Whitman (1969). The value of I_D is contained within the interval $\langle 0, 1\rangle$, where $I_D = 0$ corresponds to the most loose packing of grains, and $I_D = 1$ denotes the densest structure. It should be mentioned that the designation of loosest/densest packing of grains is not precise. Experimental procedures, suggested in geotechnical textbooks and guidelines, devoted to the determination of these extreme cases (i.e. $e_{\max}$ and $e_{\min}$) are rather rough. This problem is also difficult from the theoretical point of view, as it is possible to describe theoretically only the granular structure consisting of uniform spherical grains. Such a description is impossible in the case of actual soils.

More recent investigations, cf. Section 2, show that this traditional classification is insufficient because it is more important to define the initial state of granular soil either as contractive or dilative. This is a rather new and important classification which cannot be found in traditional soil mechanics textbooks, cf. Craig (1987) or Das (2000). In this paper, we shall not discuss this basic problem, as it needs separate treatments. Attention will be focused only on some basic statistical features of the density index, characterising investigated "Skarpa" sand.

We have divided the investigated sand into just two major groups, designated as "loose" (L) and "dense" (D) samples. Additionally, loose samples were divided onto two groups, namely very loose (L1) and loose (L2). Some statistical characteristics of the initial density index of investigated samples are shown in Table 2.

Table 2. Basic statistical characteristics of the initial density index of "Skarpa" sand samples

	Number of samples N	Range of I_D	Mean value $\overline{I_D}$	Variance s^2 ($\times 10^{-3}$)	Standard deviation s
L1	13	0.016–0.217	0.1447	1.4914	0.03862
L2	10	0.258–0.445	0.3457	2.464	0.04964
L1 + L2	23	0.016–0.445	0.2321	1.914	0.04375
D	26	0.707–0.859	0.7786	1.7934	0.00424

Respective statistical characteristics, presented in Table 2, were calculated using well known formulae:

$$\overline{I_D} = \frac{1}{N}\sum_{i=1}^{N}(I_D)_i, \tag{54}$$

$$s^2 = \frac{1}{N}\sum_{i=1}^{N}\left[\overline{I_D} - (I_D)_i\right]^2, \tag{55}$$

$$s = \sqrt{s^2}. \tag{56}$$

Fig. 7a shows the histogram, illustrating the distribution of I_D for loose samples (L1 + L2), and Figs. 7b and c show respective histograms of the distribution of I_D for soils from the groups L1 and L2. Fig. 7d shows the histogram of I_D for dense samples (designated as D).

The results shown in Fig. 7 can be summarized as follows:

a) The number of investigated samples was too small to perform a proper statistical analysis. However, in spite of this shortcoming, some basic conclusions can be drawn, which can help in formulating some hypotheses regarding the probability distribution of I_D. It is hard to find papers reporting statistical analyses of the initial state of granular soils. Some results presented in the present paper are probably the first ones touching this important problem.

b) Figs. 7a, b, c show how the method of sample preparation influences the initial relative density. The histogram from Fig. 7a has two peaks, but the histograms from Figs. 7b and c have a different character. In fact these samples were prepared using different methods. For example, very loose samples were prepared using the moist tampling method, whilst the densest samples using the water pluviation method, see Świdziński & Mierczyński (2005).

Isotropic Compression

The isotropic compression is described in Section 4. During this process, both the volumetric and deviatoric deformations develop in the sand. They are characterized by the parameters A_v and A_q, cf. Table 1. Tables 3 and 4 show basic statistical characteristics of these parameters for different initial relative densities, cf. Table 2.

Table 3. Basic statistical characteristics of the coefficient A_v

	Number of samples N	Mean A_v	Variance	Standard deviation	Range of A_v
L1	13	5.8544	0.709	0.8421	3.73–7.242
L2	10	6.202	0.6423	0.802	5.11–7.323
L1 + L2	23	6.006	0.68	0.825	3.73–7.323
D	26	3.4665	0.3358	0.5795	2.225–4.541

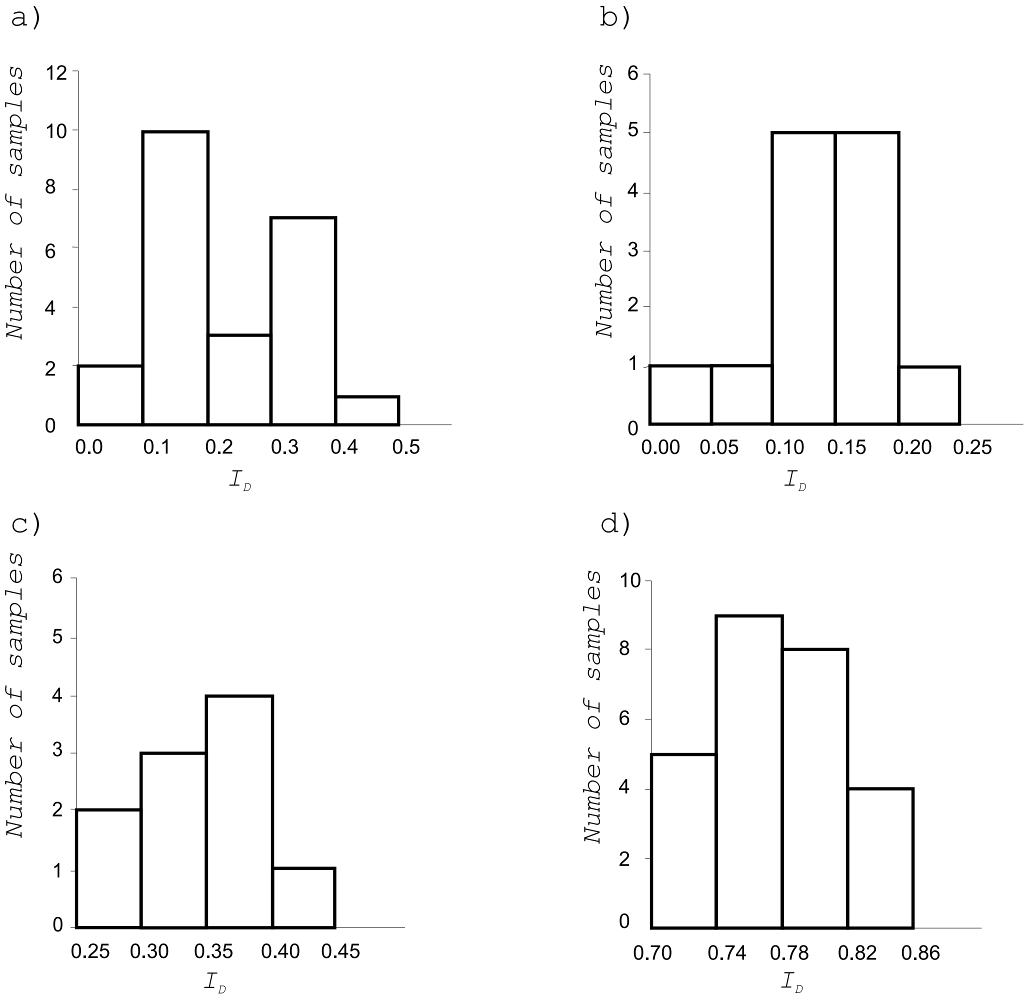

Fig. 7. Histograms illustrating the distribution of I_D of specimens of "Skarpa" sand: (a) L1 + L2 samples; (b) L1 samples; (c) L2 samples; (d) D samples, see Table 2

Table 4. Basic statistical characteristics of the coefficient A_q

	Number of samples N	Mean A_q	Variance	Standard deviation	Range of A_q
L1	12	−0.88	0.0808	0.284	−1.216 ÷ −0.36
L2	10	−1.03	0.149	0.386	−1.67 ÷ −0.29
L1 + L2	22	−0.95	0.112	0.334	−1.67 ÷ −0.29
D	27	−0.53	0.062	0.249	−1.02 ÷ −0.12

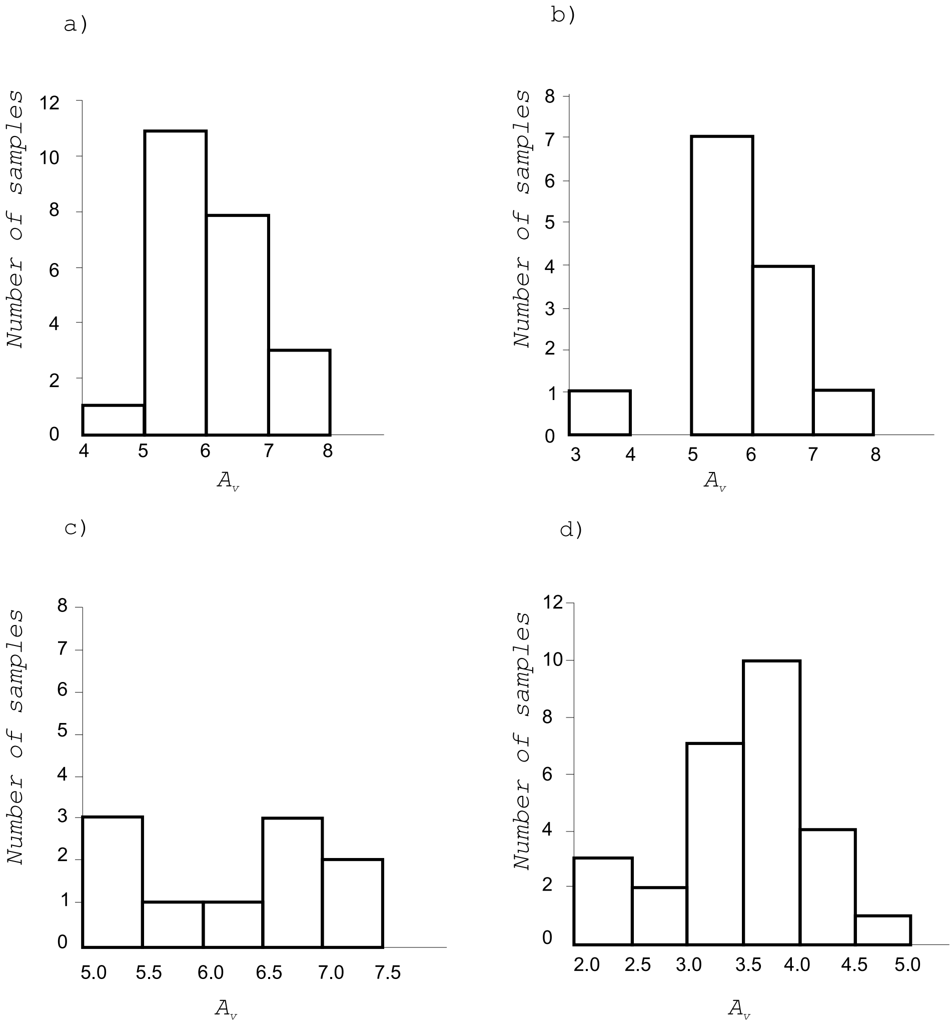

Fig. 8. Histograms illustrating the distribution of A_v of specimens of "Skarpa" sand: (a) samples L1 + L2; (b) samples L1; (c) samples L2; (d) samples D, cf. Table 3

Fig. 8a shows the histogram, illustrating the distribution of A_v for loose samples (L1 + L2), and Figs. 8b and c show respective histograms for soils from groups L1 and L2 separately. Fig. 8d shows the histogram of A_v for dense samples (D).

As in the previous case of the initial density index, the number of investigated samples was too small to draw general statistical conclusions, but the data presented may help in formulation of some hypotheses regarding, for example, probability distribution functions etc. The results shown in Tables 2–4 illustrate how uncertain may be the most simple deformation characteristics of granular soils, even determined in carefully performed experiments.

8. Discussion and Conclusions

The main results presented in this paper can be summarized as follows:

a) A simple incremental model describing pre-failure deformations of granular soils is proposed, see Eqs. (14) and (15). Functions M, N, P and Q, appearing in these equations, were determined from isotropic compression tests and from shearing at constant mean stress.

b) The above functions were determined separately for loading and unloading, both spherical and deviatoric, and for contractive and dilative samples. The instability line was built into the structure of these equations. Table 5 shows the numbers of equations defining particular functions. It should be noted that a relatively precise description of pre-failure deformations of granular soils needs a rather large number of various parameters, which are different from various "moduli" widely applied in soil mechanics.

Table 5. Numbers of equations defining particular functions appearing in incremental relations (14) and (15)

	Initial state	M	N	P	Q
Loading	contractive	18	34	21	37
	dilative	18	25, 26	21	30
Unloading	contractive	20	35	22	38
	dilative	20	28	22	32

c) Note that a new definition of loading and unloading was introduced which is different from definitions accepted in elasto-plasticity, where the loading (or yield) surface is introduced. Such a methodology leads to unobjective interpretation of those processes, as they depend on the shape of assumed yield surface.

d) The incremental equations, proposed in this paper, were applied in order to predict the soil deformations during anisotropic compression. For average soil parameters, the agreement between theoretical prediction and experimental results was satisfactory. A method of determination of K_0-line was proposed, based on the theoretical solution obtained. The direct link of this important coefficient with deformation characteristics of granular soils was shown, in contrast to commonly accepted relation with the strength characteristic, as the angle of internal friction. The results of investigations suggest that the K_0-line may perhaps be identified with the instability line.

e) Some basic statistical characteristics of the density index and the parameter describing deformations of the "Skarpa" sand during isotropic compression were presented. These data, although based on relatively small numbers of experiments from the statistical point of view, provide qualitative and quantitative information as to the character of pre-failure deformations of sands, and therefore can be used for formulating some statistical hypotheses.

f) The proposed incremental equations can be used either to calculate directly the pre-failure deformations of granular soils, or can be applied for testing various theoretical models describing pre-failure deformations of sands, as they are based on a solid empirical background. We have already used our data for testing the elasto-plastic and hypoplastic models of soils, see Sawicki (2003), Głębowicz (2006). In general, these models do not predict properly the pre-failure deformations of sand.
g) The sand investigated displays anisotropic properties as during the isotropic compression the deviatoric strains develop. Degree of such an anisotropy can be measured by the ratio $\varepsilon_q / \varepsilon_v = A_q / A_v$. This ratio is approximately –0.15 for both initially loose and dense specimens. It is a matter of individual assessment whether to neglect the deviatoric strains in theoretical modelling or not. Recall that in most theoretical models of soils the assumption of isotropy are adapted.

Acknowledgement

Research presented in this paper was financially supported by the Polish Ministry of Higher Education and Science, research grant No. 4 T07A 028 30. The author greatly appreciates this support.

References

Bolton M. (2000) *The role of micro-mechanics in soil mechanics*, Technical Report CUED/D – Soils/TR313, University of Cambridge.

Bolton M. (2001) *Micro-geomechanics*, lecture notes, University of Cambridge.

Craig R.F. (1987) *Soil Mechanics*, Van Nostrand Reinhold (UK), Wokingham.

Das B. M. (2000) *Fundamentals of Geotechnical Engineering*, Brooks/Cole, Pacific Grove, CA.

Głębowicz K. (2006) Hypoplastic modelling of pre-failure behaviour of sand against experimental data, *Archives of Hydro-Engineering and Environmental Mechanics*, **53** (1), 31–47.

Kolymbas D. (2000a) *The misery of constitutive modelling*. In: *Constitutive Modelling of Granular Materials* (D. Kolymbas, ed.), Springer, Berlin – Heidelberg – New York, 11–24.

Kolymbas, D. (2000b) *Introduction to Hypoplasticity*, Balkema, Rotterdam/Brookfield.

Lade P. V. (1992) Static instability and liquefaction of loose fine sandy slopes, *Jnl Geot. Eng.,* ASCE, **118** (1), 51–70.

Lambe T. W. and Whitman R. V. (1969) *Soil Mechanics*, John Wiley and Sons, New York – London – Sydney – Toronto.

Menzies B. K. (1988) *A computer controlled hydraulic triaxial testing system*, Advanced Triaxial Testing of Soil and Rock, ASTM STP 977, 82–94.

Poulos S. J. (1981) The steady state of deformation, *Jnl Geot. Eng.*, ASCE, **107** (5), 501–516.

Saada A. and Bianchini G. (eds.) (1989) *Constitutive Equations for Granular Non-cohesive Soils*, Balkema, Rottterdam/Brookfield.

Sawicki A. (1994) Elasto-plastic interpretation of oedometric test, *Archives of Hydro-Engineering and Environmental Mechanics,* **41** (1–2), 111–131.

Sawicki A. (2003) Cam-clay approach to modelling pre-failure behaviour of sand against experimental data, *Archives of Hydro-Engineering and Environmental Mechanics*, **50** (3), 229–249.

Sladen J. A., D'Hollander R. D. and Krahn J. (1985) The liquefaction of sands, a collapse surface approach, *Canadian Geot. Jnl*, **22**, 564–578.

Świdziński W. and Mierczyński J. (2002) On the measurement of strains in the triaxial test, *Archives of Hydro-Engineering and Environmental Mechanics*, **49** (1), 23–41.

Świdziński W. and Mierczyński J. (2005) Instability line as a basic characteristic of non-cohesive soils, *Archives of Hydro-Engineering and Environmental Mechanics*, **52** (1), 59–85.

Wood D. (1990) *Soil Behaviour and Critical State Soil Mechanics*, Cambridge University Press.

Życzkowski M. (1973) *Complex Loadings in Plasticity* (in Polish), Polish Scientific Publishers PWN, Warsaw.